

## **Supplementary Information**

**Supplement to: Latzer et al.**

**A real-world observation of patients with glioblastoma treated with a personalized peptide vaccine.**

**This supplementary information has been provided by the authors to give readers additional information about the work.**

## Supplementary Information

### Table of Contents

#### Supplementary Methods

DNA Sequencing and Bioinformatic Analyses

Immune monitoring of vaccine-induced T-cell responses

Supplementary Figure 1: Gating strategy.

Supplementary Figure 2: Results of IMM for a GBM patient.

Supplementary Figure 3: Representative pictures after the first and seventh vaccination of a GBM patient treated with a personalized neoantigen-based peptide vaccine.

Supplementary Figure 4: Evaluation of the matching quality between our cohort and public datasets.

Supplementary Table 1: Molecular characteristics of the patients' tumors assessed by next generation sequencing.

Supplementary Table 2: Number and frequency of vaccination related side effects recorded from 173 GBM patients, classified and graded according to CTCAE terminology version 5.0 (2017).

Supplementary Table 3: List of vaccinated peptides for a GBM patient.

Supplementary Table 4: Number of GBM patients available in 4 publications and treatment group for propensity score matching.

Supplementary Table 5: Multivariate Cox regression analysis.

Supplementary Table 6: MGMT and recurrence status within n=97 patients with available immune monitoring data.

Supplementary References

## Supplementary Methods

### **DNA Sequencing and Bioinformatic Analyses**

Identification of individual neoantigens was performed as previously described.<sup>1</sup> Briefly, DNA was extracted from tumor specimens (most commonly formalin-fixed paraffin-embedded (FFPE) material) and from EDTA blood. Sequencing libraries were prepared from each sample using either the Agilent SureSelect workflow (Agilent, Santa Clara, CA) or the Twist enrichment workflow (Twist Biosciences, San Francisco, CA), with varying exome enrichment kits (SureSelect Human Exome versions 5, 6, and 7; Twist Comprehensive Exome version 1; CeGaT Exome Extra versions 1 and 2). Library preparation and capture were performed according to the manufacturer's instructions and paired-end sequencing was performed on a HiSeq2500 or NovaSeq6000 (Illumina, San Diego, CA).

Sequence variants were called with a minimum variant allele frequency of 5%. Resulting variants were annotated with population frequencies from public databases (dbSNP, GnomAD) and an internal database, with functional predictions from dbNSFP (3), with publications from HGMD® and with transcript information from Ensembl, RefSeq and CCDS. Blood and tumor data were analyzed comparatively to determine germline/somatic status for each variant.

Tumor mutational burden (TMB) was defined as the number of somatic single-nucleotide variants (SNVs), InDels and essential splice site variants (NAF  $\geq 0.1$ ) per megabase of coding DNA. Somatic variants with an in-house frequency of  $\geq 1\%$  were not included. TMB was classified as high, when  $\geq 10$  Mut/Mb were present in the tumor.<sup>2,3</sup>

For microsatellite instability (MSI), the prediction was carried out using MANTIS.<sup>4</sup>

Homologous recombination deficiency (HRD) score was calculated as the sum of the markers described previously.<sup>5,6,7</sup> The cut-off of a positive HRD-score was set to 30 based on internal validation approaches.

The TMZ signature was defined as C>T mutations in the following triplet constellations: ACC, ACT, CCC, CCT, GCC, GCT, TCC and TCT (SBS11).<sup>8</sup> The cut-off of a positive TMZ signature was set to 15% based on internal validation approaches.

### **Peptide prediction**

Identified somatic variants and in-phase germline variants were translated into peptide sequences. MHC class I epitopes were predicted using SYFPEITHI, netMHC-4.0 and netMHCpan-4.1.<sup>9-11</sup> Peptides containing somatic variants that are classified as binder by at least one prediction method were further evaluated. The respective thresholds for classification as binder were defined as <500 nM for netMHC and netMHCpan as well as >50% of maximal score for SYFPEITHI. Peptides resembling a wildtype sequence in the human proteome (based on UniProtKB/Swiss-Prot, human, 9/7/14) were excluded.

An in-house developed and proprietary neoantigen selection algorithm was used to select neoepitopes. Putative HLA class I epitopes with a high HLA class I binding prediction score derived from variants with high allele frequencies were selected. Peptides predicted to bind to different HLA class I molecules of the patient were prioritized. Peptides which are predicted to bind to several HLA types were further prioritized. Putative HLA class II epitopes with a length of +/-17 amino acids were designed to contain variants with high allele frequencies. Peptides spanning variants in possible tumor drivers were prioritized. Peptides with a high percentage of hydrophobic amino acids, peptides with a high probability for gelation or dimerization were excluded to avoid solubility problems in an aqueous solution and problems

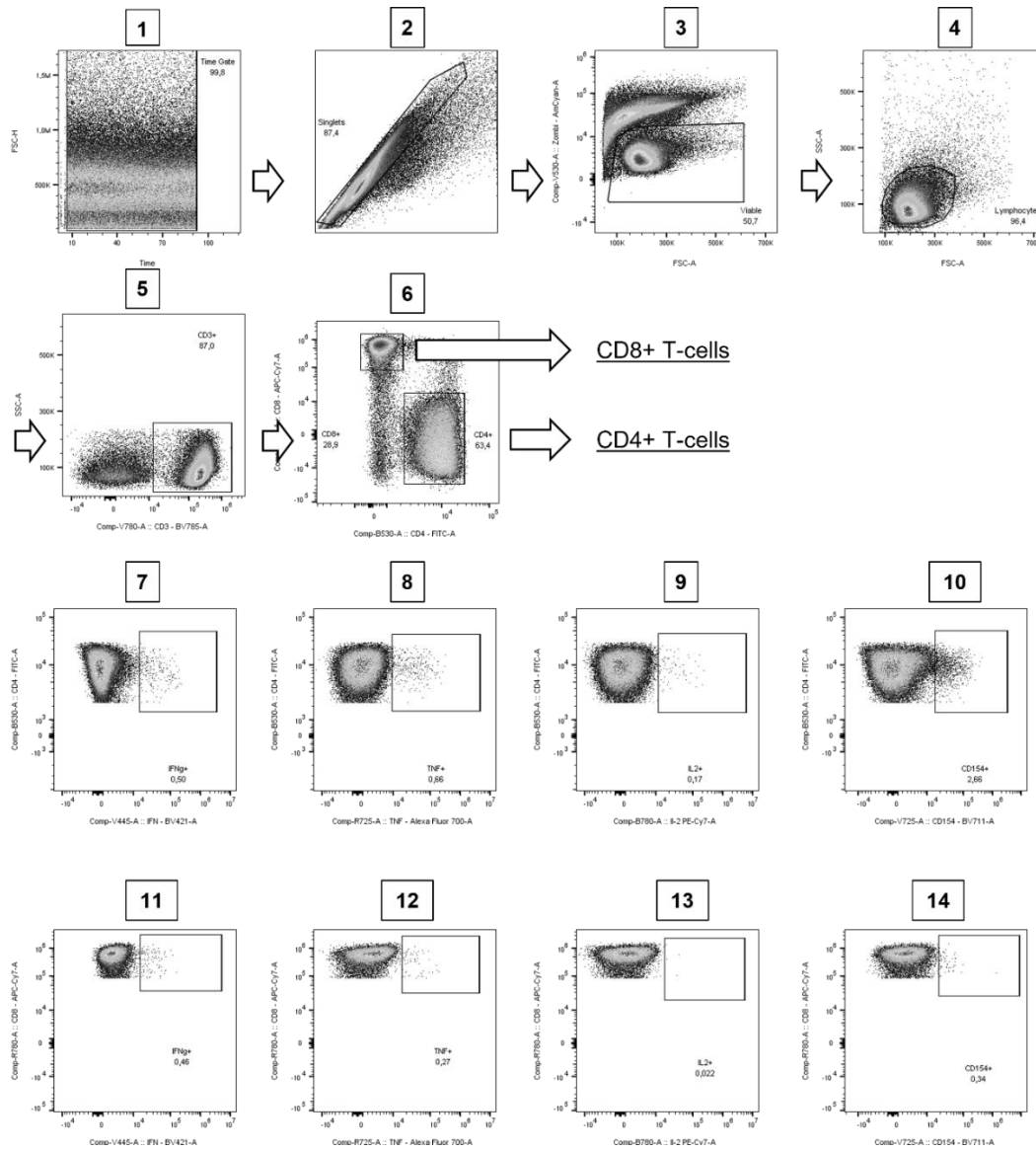
during synthesis. Peptides derived from genes most probably not expressed in the patient's tumor entity were excluded. For this purpose, expression data for the respective variant were analyzed using RNA sequencing data of the tumor sample. The bioinformatically identified somatic variants corresponding to all selected peptides were manually reviewed in the sequencing data and filtered for false positives.

### **Immune monitoring of vaccine-induced T-cell responses**

Blood mononuclear cells (PBMC) including T-cells were isolated by Ficoll Hypaque and cryopreserved in MACS® Freezing Solution (Miltenyi Biotec) for later use. Cryopreserved PBMC were thawed and cells were cultured overnight to recover, stimulated with patient-individual mutated peptides and cultured 12 days in the presence of IL-2 and IL-7. For analysis, cells were restimulated for  $12 \pm 2$  hours with peptides or incubated with medium only (unstimulated negative control) or 10  $\mu$ /mL CytoStim™ (Miltenyi Biotec) in presence of Golgi-Plug (BD biosciences) at a concentration of 1  $\mu$ /ml. After restimulation, the final readout was an Intracellular Cytokine Staining (ICS). After cultivation, cells were washed twice followed by extracellular staining with fluorochrome-conjugated antibodies titrated to their optimal concentrations: CD3-BV785 (clone UCHT1; BioLegend; dilution: 1/33), CD4-FITC (clone RPA-T4; BioLegend; dilution: 1/100), CD8-APC/Cyanine (clone SK1; BioLegend; dilution: 1/50), Zombi Aqua Dye (BioLegend; dilution: 1/200). After extracellular staining, cells were fixed and permeabilized (BD biosciences), followed by an intracellular staining with the following antibodies: IFN-BV421 (clone 4S.B3; BioLegend; dilution: 1/50), TNF-AlexaFluor700 (clone MAb11; BioLegend; dilution: 1/50), IL-2-PE/Cy7 (clone MQ1-17H12; BioLegend; dilution: 1/50) and CD154 – BV711 (clone 24-31; BioLegend; dilution: 1/25). Finally, cells were measured on a Novocyte

3005R cytometer (ACEA biosciences). Peptide-specific responses were evaluated using the stimulation index (SI). The stimulation index is the calculated ratio of polyfunctional activated CD4+ or CD8+ T-cells (positive for at least two markers of IFN- $\gamma$ , TNF- $\alpha$ , IL-2 and/or CD154) in the peptide-stimulated sample to the negative control sample (DMSO). Neoantigen-specific T-cells are defined as being present for SI  $\geq$ 2.

## Supplementary Figure 1: Gating strategy.



We included only cells that were constantly measured over time (1; Forward-scatter (FSC)-H versus Time). Herein, single (2; FSC-A versus FSC-H), viable (3; Zombie Aqua-negative cells), lymphocytes (4; FSC-A versus Side-scatter (SSC)-A) and CD3+ T-cells (5) were selected. CD3+ T-cells were further discriminated in CD4+ or CD8+ T-cells (6). Within both CD4+ (7-10) and CD8+ T-cells (11-14), we determined the production/expression of the functional markers IFN- $\gamma$  (7, 11), TNF (8, 12), IL-2 (9, 13) and CD154 (10, 14).



Supplementary Figure 2: Results of IMM for a GBM patient.

Peptide-specific immune responses						04.11.2019 (V1) + 06.11.2019 (V2)		19.02.2020 (V7)	
No	Peptide	Gene and Coding info	NAF (DNA)	NAF (RNA)	HLA	CD4	CD8	CD4	CD8
1	YSFGVTCV	EGFR:NM_005228:c.C866T:p.A289V	0.89	0.92	HLA-A*02:01, HLA-C*03:03	-	-	-	+
2	LLGRNSFEVHV	TP53:NM_000546:c.G818A:p.R273H	0.75	0.83	HLA-A*02:01	-	-	SI: 2.9 (0.3%)	
3	NLINEDIESA	EPS8:NM_004447:c.G530A:p.S177N	0.26	0.22	HLA-A*02:01	-	-	+ SI: 2.4 (0.8%)	-
4	KQKPIITEKL	RFC4:NM_181573:c.T973C:p.S325P	0.32	0.36	HLA-B*13:02, HLA-B*15:01				
5	FSQKSGSAF	DST:NM_001144769:c.C509T:p.S170F	0.42	0.59	HLA-B*15:01, HLA-C*03:03, HLA-C*06:02	-	-	- SI: 77.9 (13.0%)	++++
6	HQKIHMGVKPY	ZNF540:NM_152606:c.C1721T:p.T574M	0.30	0.80	HLA-B*15:01				
7	SGPPVLGGKSNSNSSGG	SH2B1:NM_001145795:c.C591G:p.N197K	0.41	0.63	Class II	-	-	-	+++
8	YQAEPNSSFMAQREENVP	PTPRN2:NM_001308267:c.G2290A:p.V764M	0.28	0.44	Class II				
9	IKAKSQFKWRSTANNVE	AP1M1:NM_001130524:c.C907T:p.R303W	0.23	0.21	Class II				
10	RVRPRAPATRVPGPGPS	DACT3:NM_001301046:c.G1489A:p.A497T	0.24	0.14	Class II	-	-	SI: 7.9 (1.9%)	

T-cell responses for patients 1, 2 and 3 respectively, during and following peptide vaccine treatment. Vn denotes day of/after vaccination. HLA: HLA which was predicted to bind the peptide. NAF: Novel allele frequency, frequency with which the mutated allele was occurring in the tumor (1 corresponds to 100%). The observed frequencies are influenced by the tumor content of the analysed sample and hence do not correlate directly to the mutation frequency of the tumor. SI: Stimulation index, ratio of polyfunctional activated CD4+ or CD8+ T-cells (positive for at least two activation markers of CD154, IFN- $\gamma$ , TNF and/or IL-2) in the peptide-stimulated sample compared to the unstimulated control. Additionally, the percentage of activated CD4+ or CD8+ T-cells (positive for at least one activation marker of CD154, IFN- $\gamma$ , TNF and/or IL-2) above background and after in vitro amplification is given. The percentage does not directly reflect the frequencies in vivo. Please note that SI and % values should be considered only in combination and not independently from each other. SI  $\geq$ 2: weak response (+), SI  $\geq$ 3: positive response (++), SI  $\geq$ 5: strong response (+++), SI  $\geq$ 10: very strong response (++++).

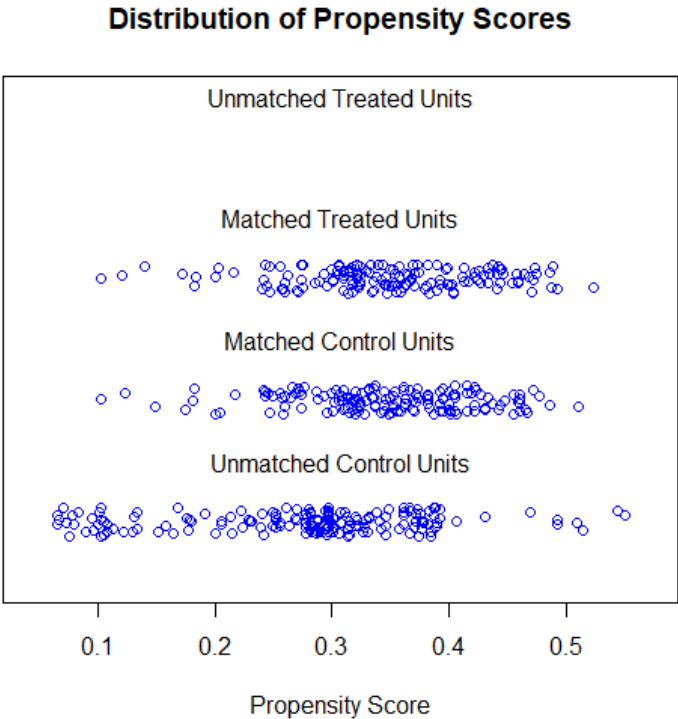
Supplementary Figure 3: Representative pictures after the first and seventh vaccination of a GBM patient treated with a personalized neoantigen-based peptide vaccine.

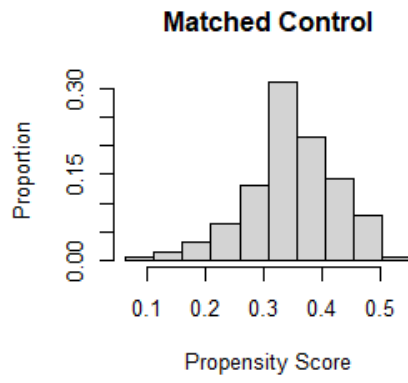
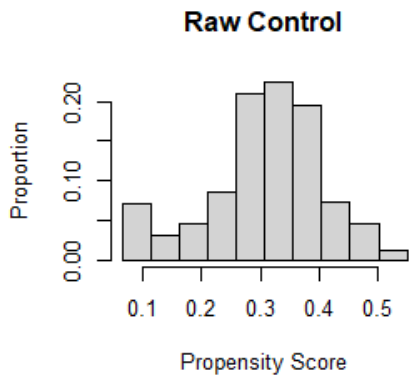
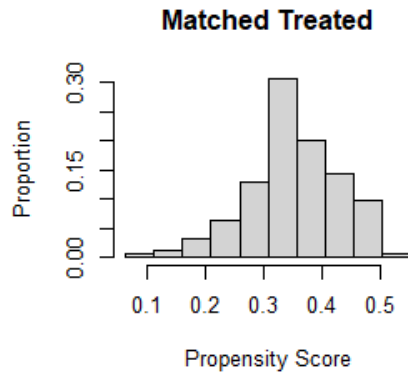
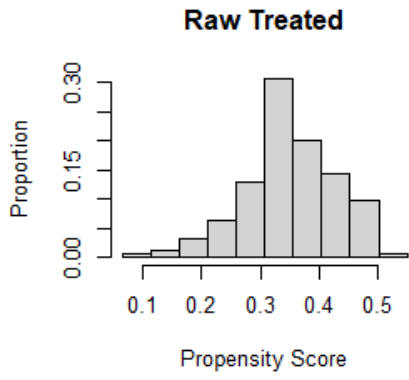


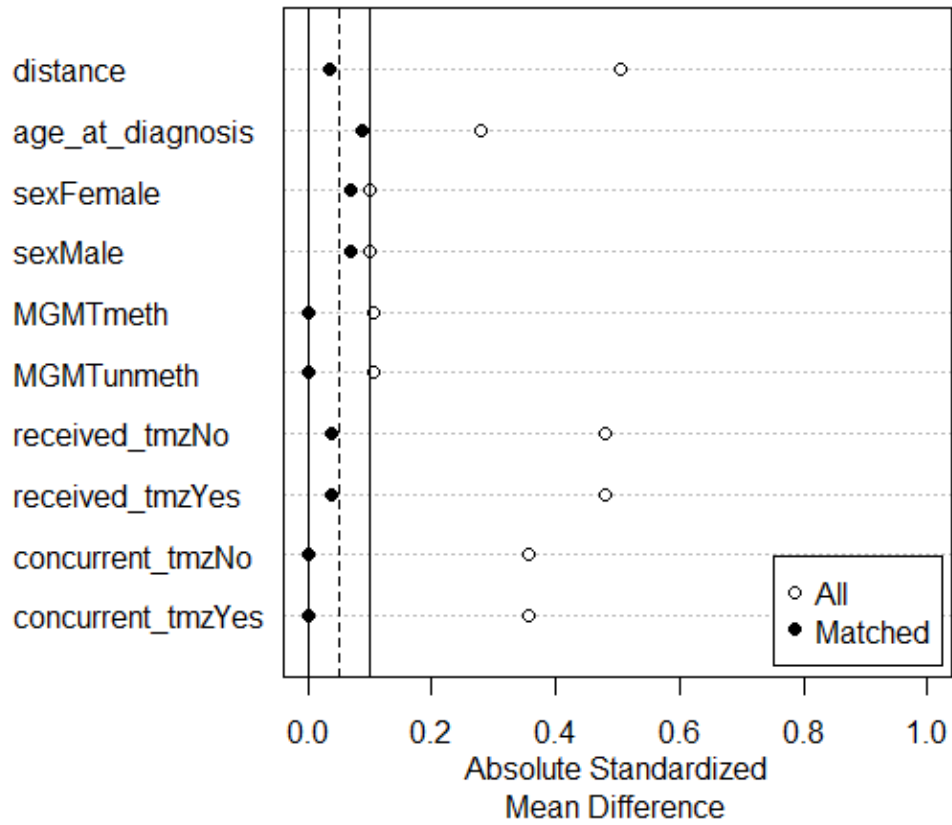
Representative pictures after the first and seventh vaccination of a GBM patient treated with a personalized neoantigen-based peptide vaccine.

Picture of the injection site after the first (left) and the seventh vaccination (right, about 3 months after the first vaccination) showing vaccine tolerability.

Supplementary Figure 4: Evaluation of the matching quality between our cohort and public datasets.

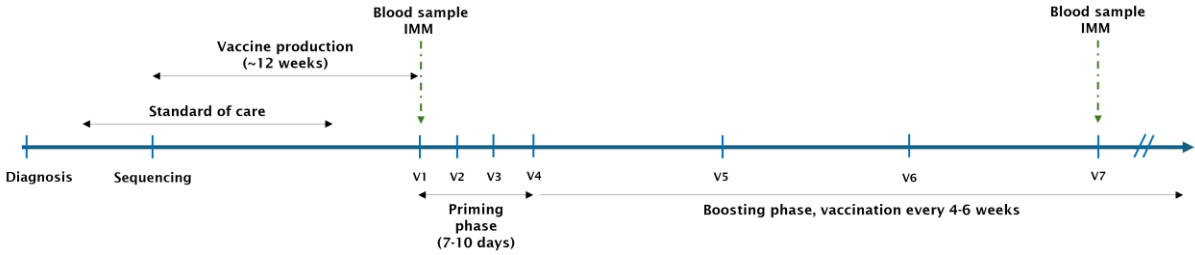






Evaluation of the matching quality between our cohort and public datasets. The jitter plot and histograms showed the balance of propensity scores before and after matching. The balance of individual variables was evaluated using the standardized mean difference and visualized by the variable balance plot.

Supplementary Figure 5: Vaccination protocol.



Abbreviations: IMM, immune monitoring; V, vaccination

Supplementary Table 1: Molecular characteristics of the patients' tumors assessed by next generation sequencing.

	Patients	%
Germline variants associated with hereditary tumor predisposition	31	18%
Pharmacogenetic variants ( <i>DPYD</i> , <i>G6PD</i> , <i>RYR1</i> , <i>TPMT</i> , <i>UGT1A1</i> )	27	16%
Tumor mutational burden of at least 10 variants/megabase	7	4%
Microsatellite instability	4	2%
Homologous recombination deficiency score $\geq 30$	32	19%
Mutations in genes involved in DNA repair mechanisms	12	7%
Homozygous <i>CDKN2A/B</i> deletion	68	39%
<i>RB1</i> inactivating alteration	24	14%
<i>CDK4/CDK6</i> amplification	29	17%
<i>MDM2/MDM4</i> amplification	24	14%
<i>TP53</i> mutation	50	29%
<i>PTEN</i> inactivating alteration	60	35%
<i>NF1</i> loss of function	31	18%
<i>ATRX</i> mutation	2	1%

Only mutations that were classified as functionally relevant were considered. For copy number alterations, only amplifications with a strength of  $> 5$  or homozygous deletions were considered. Alteration is defined as either mutation and/or deletion.



Supplementary Table 2: Number and frequency of vaccination related side effects recorded from 173 GBM patients, classified and graded according to CTCAE terminology version 5.0 (2017).

<b>CTCAE Term</b>	<b>CTCAE Grade 1-2 N (%)</b>	<b>CTCAE Grade 3 N (%)</b>	<b>CTCAE Grade 4 N (%)</b>
No AE: N=654 (42%)	---	---	---
Injection site reaction	586 (38%)	1 (0.1%)	---
Pruritus	32 (2%)	---	---
Flu-like symptoms	3 (0.2%)	---	---
Fever	1 (0.1%)	---	---
Chills	3 (0.2%)	---	---
Headache	3 (0.2%)	---	---
Nausea	2 (0.1%)	---	---
Fatigue	6 (0.4%)	---	---
Dizziness	3 (0.2%)	---	---
Hypertension	2 (0.1%)	---	---
Allergic reaction	5 (0.3%)	1 (0.1%)	---
Anaphylaxis	4 (0.3%)	2 (0.1%)	---

Supplementary Table 3: List of vaccinated peptides for a GBM patient.

Peptide	AA sequence	Gene and coding information	HLA	NAF DNA
1	YSFGVTCV	EGFR:NM_005228:c.C866T:p.A289V	A*02:01, C*03:03	0.89
2	LLGRNSFEVHV	TP53:NM_000546:c.G818A:p.R273H	A*02:01	0.75
3	NLINEDIESA	EPS8:NM_004447:c.G530A:p.S177N	A*02:01	0.26
4	KQKPIITEKL	RFC4:NM_181573:c.T973C:p.S325P	B*13:02, B*15:01	0.32
5	FSQKSGSAF	DST:NM_001144769:c.C509T:p.S170F	B*15:01, C*03:03, C*06:02	0.42
6	HQKIHMGVKPY	ZNF540:NM_152606:c.C1721T:p.T574M	B*15:01	0.30
7	SGPPVLGGKSNSNSSGG	SH2B1:NM_001145795:c.C591G:p.N197K	Class II	0.41
8	YQAEPNSSFMAQREENVP	PTPRN2:NM_001308267:c.G2290A:p.V764M	Class II	0.28
9	IKAKSQFKWRSTANNVE	AP1M1:NM_001130524:c.C907T:p.R303W	Class II	0.23
10	RVRPRAPATRVPGPGPS	DACT3:NM_001301046:c.G1489A:p.A497T	Class II	0.24

Abbreviations: AA, amino acid; HLA, human leukocyte antigen, which was predicted to bind the peptide; NAF, novel allele frequency, frequency with which the mutated allele was occurring in the tumor (1 corresponds to 100%). The observed frequencies are influenced by the tumor content of the analyzed sample and hence do not correlate directly to the mutation frequency of the tumor.

Supplementary Table 4: Number of patients included for the propensity score matching from public datasets and our cohort.

<b>Study</b>	<b>Number of patients</b>	<b>Median overall survival in months and 95% CI</b>	<b>Number of patients alive at publication data cutoff</b>	<b>Median follow up time in months and 95% CI</b>
GLASS Consortium, Nature 2019 <sup>12</sup>	86	22, [21, 27]	4 (4.7%)	NA, [NA, NA]
TCGA, Cell 2013 <sup>13</sup>	125	17.8, [16.5, 20.7]	19 (15.2%)	92.6, [92.6, NA]
MSK, Clin Cancer Res 2019 <sup>14</sup>	69	36.1, [25.3, 59.4]	24 (34.8%)	58.6, [39.4, NA]
Lakomy, Frontiers in Oncology 2020 <sup>15</sup>	44	23.3, [17.4, 30.9]	9 (20.5%)	34.8, [32.9, NA]
Total patient number in 4 publications	324	21.7, [20.8, 23.5]	56 (17.3%)	61.2, [58, NA]]
<i>Our treatment cohort</i>	159	31.1, [25, 36.5]	86 (54%)	31.4, [26.8, 34.1]

Supplementary Table 5: Multivariate Cox regression analysis.

<b>Variable</b>	<b>Reference level</b>	<b>p-value</b>	<b>Hazard ratio</b>	<b>95% CI</b>	<b>p-value of Schoenfeld residual test</b>
Age at diagnosis	1 year younger	3.8e-04	1.03	[1.01, 1.04]	0.92
Gender	female	7.6e-02	1.33	[0.97, 1.82]	0.76
MGMT status	methylated	6.6e-06	1.97	[1.47, 2.65]	0.81
Received Temozolomide	no	1.9e-02	0.35	[0.15, 0.84]	0.87
Received concurrent chemoradiotherapy	no	2.9e-01	0.76	[0.46, 1.26]	0.68
Patient group	untreated	4.0e-03	0.65	[0.48, 0.87]	0.83

The p-values are based on 2-sided tests.

Supplementary Table 6: MGMT and recurrence status within n=97 patients with available immune monitoring data.

1. MGMT status\*

	methylated	unmethylated
iNR	8	11
iR	46	27

2. Recurrence before 1<sup>st</sup> vaccination

	recurrent	Not recurrent
iNR	12	8
iR	35	42

3. Immunosuppressant intake

	Received immunosuppressant	Did not receive
iNR (n = 20)	8	12
R (n = 77)	37	40

Abbreviations: iNR, immunological non-responders; iR = immunological responders

\*MGMT information is missing for n=5 patients.

There was no association between MGMT status ( $P=0.12$ ; Fisher's exact test, 2-sided), recurrence status ( $P=0.32$ ) or immunosuppressant intake ( $P=0.62$ ) and induced T-cell responses.

## Supplementary References

1. Blumendeller C, Boehme J, Frick M, et al. Use of plasma ctDNA as a potential biomarker for longitudinal monitoring of a patient with metastatic high-risk upper tract urothelial carcinoma receiving pembrolizumab and personalized neoepitope-derived multi-peptide vaccinations: a case report. *J Immunother Cancer*. 2021 Jan;9(1):e001406. doi: 10.1136/jitc-2020-001406. PMID: 33431630; PMCID: PMC7802705.
2. Hellmann MD, Ciuleanu TE, Pluzanski A, et al. Nivolumab plus Ipilimumab in Lung Cancer with a High Tumor Mutational Burden. *N Engl J Med*. 2018 May 31;378(22):2093-2104. doi: 10.1056/NEJMoa1801946. Epub 2018 Apr 16. PMID: 29658845; PMCID: PMC7193684.
3. Reck M, Schenker M, Lee KH, et al. Nivolumab plus ipilimumab versus chemotherapy as first-line treatment in advanced non-small-cell lung cancer with high tumour mutational burden: patient-reported outcomes results from the randomised, open-label, phase III CheckMate 227 trial. *Eur J Cancer*. 2019 Jul;116:137-147. doi: 10.1016/j.ejca.2019.05.008. Epub 2019 Jun 11. PMID: 31195357.
4. Kautto EA, Bonneville R, Miya J, et al. Performance evaluation for rapid detection of pan-cancer microsatellite instability with MANTIS. *Oncotarget*. 2017 Jan 31;8(5):7452-7463. doi: 10.18632/oncotarget.13918. PMID: 27980218; PMCID: PMC5352334.
5. Birkbak NJ, Wang ZC, Kim JY, et al. Telomeric allelic imbalance indicates defective DNA repair and sensitivity to DNA-damaging agents. *Cancer Discov*. 2012 Apr;2(4):366-375. doi: 10.1158/2159-8290.CD-11-0206. Epub 2012 Mar

22. Erratum in: *Cancer Discov.* 2013 Aug;3(8):952. PMID: 22576213; PMCID: PMC3806629.
6. Abkevich V, Timms KM, Hennessy BT, et al. Patterns of genomic loss of heterozygosity predict homologous recombination repair defects in epithelial ovarian cancer. *Br J Cancer.* 2012 Nov 6;107(10):1776-82. doi: 10.1038/bjc.2012.451. Epub 2012 Oct 9. PMID: 23047548; PMCID: PMC3493866.
7. Popova T, Manié E, Rieunier G, et al. Ploidy and large-scale genomic instability consistently identify basal-like breast carcinomas with BRCA1/2 inactivation. *Cancer Res.* 2012 Nov 1;72(21):5454-62. doi: 10.1158/0008-5472.CAN-12-1470. Epub 2012 Aug 29. PMID: 22933060.
8. Degasperi A, Zou X, Amarante TD, et al. Substitution mutational signatures in whole-genome-sequenced cancers in the UK population. *Science.* 2022 Apr 22;376(6591):science.abl9283. doi: 10.1126/science.abl9283. PMID: 35949260; PMCID: PMC7613262.
9. Rammensee H, Bachmann J, Emmerich NP, Bachor OA, Stevanović S. SYFPEITHI: database for MHC ligands and peptide motifs. *Immunogenetics.* 1999 Nov;50(3-4):213-9. doi: 10.1007/s002510050595. PMID: 10602881.
10. Andreatta M, Nielsen M. Gapped sequence alignment using artificial neural networks: application to the MHC class I system. *Bioinformatics.* 2016 Feb 15;32(4):511-7. doi: 10.1093/bioinformatics/btv639. Epub 2015 Oct 29. PMID: 26515819; PMCID: PMC6402319.
11. Reynisson B, Alvarez B, Paul S, Peters B, Nielsen M. NetMHCpan-4.1 and NetMHCIIpan-4.0: improved predictions of MHC antigen presentation by concurrent motif deconvolution and integration of MS MHC eluted ligand data.

Nucleic Acids Res. 2020 Jul 2;48(W1):W449-W454. doi: 10.1093/nar/gkaa379.

PMID: 32406916; PMCID: PMC7319546.

12. Barthel FP, Johnson KC, Varn FS et al. Longitudinal molecular trajectories of diffuse glioma in adults. *Nature* 576, 112–120 (2019).

<https://doi.org/10.1038/s41586-019-1775-1>

13. Brennan CW, Verhaak RG, McKenna A, et al. The somatic genomic

landscape of glioblastoma. *Cell*. 2013 Oct 10;155(2):462-77. doi:

10.1016/j.cell.2013.09.034. Erratum in: *Cell*. 2014 Apr 24;157(3):753. PMID:

24120142; PMCID: PMC3910500.

14. Jonsson P, Lin AL, Young RJ, et al. Genomic Correlates of Disease

Progression and Treatment Response in Prospectively Characterized

Gliomas. *Clin Cancer Res*. 2019 Sep 15;25(18):5537-5547. doi:

10.1158/1078-0432.CCR-19-0032. Epub 2019 Jul 1. PMID: 31263031;

PMCID: PMC6753053.

15. Lakomy R, Kazda T, Selingerova I et al. Real-World Evidence in Glioblastoma:

Stupp's Regimen After a Decade. *Front Oncol*. 2020 Jul 3;10:840. doi:

10.3389/fonc.2020.00840. PMID: 32719739; PMCID: PMC7348058.